Clinical Science (2023) **137** 47–63
https://doi.org/10.1042/CS20220513

PORTLAND PRESS

Research Article

Sexual dimorphism in acute myocardial infarction-induced acute kidney injury: cardiorenal deteriorating effects of ovariectomy in premenopausal female mice

Nada J. Habeichi[1,2,3], Rana Ghali[2,*], Ali Mroueh[2,*], Abdullah Kaplan[2], Cynthia Tannous[2], Abdo Jurjus[4], Ghadir Amin[2,3], Mathias Mericskay[1], George W. Booz[5], Ahmed El-Yazbi[6,7] and Fouad A. Zouein[1,2,3,5]

[1]Department of Signaling and Cardiovascular Pathophysiology, Université Paris-Saclay, Inserm, UMR-S 1180, Châtenay-Malabry, France; [2]Department of Pharmacology and Toxicology, American University of Beirut, Faculty of Medicine, Beirut, Lebanon; [3]The Cardiovascular, Renal, and Metabolic Diseases Research Center of Excellence, American University of Beirut Medical Center, Beirut, Lebanon; [4]Department of Anatomy, Cell Biology, and Physiology, American University of Beirut Medical Center, Beirut, Lebanon; [5]Department of Pharmacology and Toxicology, School of Medicine, University of Mississippi Medical Center, Jackson, MS, U.S.A.; [6]Department of Pharmacology and Toxicology, Faculty of Pharmacy, Alexandria University, Alexandria, Egypt; [7]Department of Pharmacology and Toxicology, Faculty of Pharmacy, Alamein International University, Alexandria, Egypt

Correspondence: Fouad A. Zouein (fz15@aub.edu.lb) or Ahmed El-Yazbi (ahmed.fawzy.aly@alexu.edu.eg) or Mathias Mericskay (mathias.mericskay@inserm.fr)

OPEN ACCESS

Acute kidney injury (AKI) is a common complication of cardiovascular diseases (CVDs) in both males and females, increasing mortality rate substantially. Premenopausal females appear to be more protected, suggesting a potential protective role of female sex hormones. Here, we tested the hypothesis that ovariectomy (OVX) eliminates the beneficial effect of female sex on renal protection following acute myocardial infarction (MI). Seven days post-MI, both sexes exhibited worsened kidney function and a substantial decrease in total kidney NAD levels. Unlike MI female mice, MI males showed exacerbated morphological alterations with increased proinflammatory, proapoptotic, and profibrotic biomarkers. The expression of NAD^+ biosynthetic enzymes NAMPT and NMRK-1 was increased in MI females only, while males showed a substantial increase in NAD^+ consuming enzyme PARP-1. OVX did not eliminate the female-sex protection of glomerular morphology but was associated with swelling of proximal convoluted tubules with MI as in males. With OVX, MI females had enhanced proinflammatory cytokine release, and a further decrease in creatinine clearance and urine output was observed. Our findings suggest that MI induced AKI in both sexes with pre-menopausal female mice being more protected. Ovariectomy worsens aspects of AKI in females after MI, which may portend increased risk for development of chronic kidney disease.

Introduction

Cardiovascular diseases (CVDs) remain the leading cause of death in both sexes with tremendous health and economic burdens worldwide [1–3]. According to the world health organization (WHO), 4 out of 5 CVD deaths are attributed to myocardial infarction (MI) and stroke (http://www.who.int/cardiovascular_diseases/en/) [4]. Epidemiological studies revealed that one American is subject to an MI every 60 s [5]. Sex discrepancies in CVDs have been well established, with premenopausal women being less prone to develop MI compared with age-matched men [2,6]. MI prevalence, however, increases with age to reach comparable levels after menopause [7,8]. For instance, the female-to-male MI risk ratio is 1:10 under the age of 45, while increasing dramatically to 1:2 over the age of 75 [9].

*These authors contributed equally to this work.

Received: 04 August 2022
Revised: 13 December 2022
Accepted: 14 December 2022

Accepted Manuscript online: 15 December 2022
Version of Record published: 05 January 2023

Clinical Science (2023) **137** 47–63
https://doi.org/10.1042/CS20220513

Of note, patients diagnosed with MI are not only at a 30-fold increase in risk of heart failure development but also at a 25-fold increase in risk of cardiorenal syndrome (CRS) through the cardiorenal inter-relationship, increasing therefore the mortality rate substantially [10,11]. In fact, MI-induced left ventricle (LV) systolic dysfunction leads to decreased stroke volume (SV) and cardiac output (CO), and a subsequent decline in renal perfusion [12–14]. In addition to altered cardiac hemodynamics, systemic inflammation post-MI can aggravate kidney damage progression and development independently of compromised cardiac systolic function [15]. Evidence indicates that acute kidney injury (AKI) is a common occurrence with ST-segment elevation MI (STEMI) and is correlated with poor prognosis [16].

Accumulating preclinical and clinical studies report sexual dimorphism in kidney damage pathogenesis, being less frequent in premenopausal females [17,18]. A recent study reported that AKI occurs more often in women, presumably postmenopausal, than in men with MI undergoing percutaneous coronary intervention (PCI), although the basis for this was not defined [19].

Sex differences are potentially attributable to the nephroprotective effects of endogenous estrogen, 17β Estradiol (E2) [20–22]. To date, our understanding of the impact of cardiac dysfunction as early as 7 days post-MI on male and female kidney damage is very limited. In the present study, we asked the question of whether the sexual dimorphism in MI-induced AKI between male and age-matched premenopausal female mice is reversed by ovariectomy.

Materials and methods

Additional methods may be found in the Supplementary Material.

Animal use

C57BL6/J mice were employed in the present study according to the experimental protocol approved by the Institutional Animal Care and Use Committee (IACUC) of the American University of Beirut (AUB) and in compliance with the National Institutes of Health Guide for the Care and Use of Laboratory Animals, 8th edition [23]. The approved IACUC protocol number was #18-2-RN560. Five months old age-matched male and female mice (equivalent to a 30-year-old human) were maintained in the animal care facility of the AUB Medical Center under optimum conditions with 12 light/12 dark hours cycle and access to unlimited water and standard chow. Surgical procedures and experiments with animals were performed in the animal care facility of the American University of Beirut Medical Center (AUBMC).

Experimental design

Five months old C57BL6/J mice were allocated into five groups: male control (MC), female control (FC), MI-male (MMI), MI-female (FMI), and ovariectomized MI-female (FMIOVX). For MI groups, MI was induced by ligation of the left anterior descending (LAD) coronary artery. Mice of both sexes were sacrificed 7 days post-MI. Bilaterally ovariectomized female mice (FOVX) were caged individually for 3 weeks post-operation and monitored on a daily basis until full recovery. At the end of week 3, FOVX mice underwent MI (FMIOVX) and were killed 7 days later. Thirty minutes prior to sacrifice, 100 μl heparin (heparin sodium 1000 IU/ml) was administrated to mice and deep anesthesia induced with 4% isoflurane. Cardiac puncture was used to collect blood followed by centrifugation at 2200 rpm for 10 min; plasma was collected, mixed with protease inhibitor cocktail, and flash frozen in liquid nitrogen and stored at −80°C. Mice were then subjected to cervical dislocation. Left kidney was harvested and immediately placed into a cryotube in liquid nitrogen followed by storage at –80°C for molecular work. Right kidney was harvested into 4% zinc formalin tubes for histology.

Surgical procedures

MI was induced by permanent ligation of the LAD coronary artery. In order to reduce any surgical complication, HR, respiratory rate, and body temperature were monitored throughout the procedure. Analgesia and general anesthesia were induced by tramadol (0.05–0.1 mg/kg i.p.) and isoflurane (2–3% in oxygen) inhalation, respectively, and prior to surgery. Anesthesia-induced hypothermia was controlled by a heating pad. Orotracheal intubation was induced by placing a Y-tube into the trachea and connecting it to a mini-automated ventilator (Harvard Apparatus) in order to maintain normal respiratory rate. LV, left atria, and LAD coronary artery were exposed by excising between the ribs of the left thorax. MI was induced by LAD ligation with 7-0 polypropylene suture at 1-3 mm underneath the left atrium appendage, then the chest was sutured and the mouse placed on a warm pad for recovery. Successful MI was established by blanching of tissue downstream of the ligation, by ECG, and by echocardiography 24 h post-surgery. After grooming freely, MI mice were caged back and monitored daily for full recovery. Control mice underwent sham

Table 1 List of antibodies for WB analysis

Antibodies	Catalog number	Dilution
IL-1β	Abcam; cat# ab9722	1/500
Caspase-3	Abcam; cat# ab4051	1/500
IL-4	Abcam; cat# ab9728	1/1000
α-SMA	Abcam; cat# ab5694	1/200

surgery. For ovariectomy, mice were anesthetized with 2% isoflurane, placed in a supine position, and maintained on a heating pad to avoid heat loss. The ventral area was shaved, cleaned with 70% ethanol, and the peritoneal cavity accessed with a 1 cm midline incision performed below the bottom of the ribcage. Adipose tissue located under the right kidney was pulled away to locate and identify the uterine horn and the right ovary. Using blunt forceps, the ovarian fat surrounding the ovaries was retracted and the oviduct exposed and isolated with a 6.0 prolene suture to prevent bleeding. Using small sterile scissors, the oviduct was gently severed and the uterine horn returned back to the abdominal cavity. The same procedure was repeated to remove the left ovary. The peritoneum and skin were closed in layers using sterile 6.0 prolene sutures. Mice were finally housed on cleaned and dried bedding and allowed to recover for a period of 3 weeks before LAD ligation. Estrogen levels were measured 4 weeks following ovariectomy (Supplementary Table S1).

Histology

Glomerular retraction was assessed using hematoxylin and eosin (H&E) staining. Briefly, kidney tissues were fixed with 4% formalin, dehydrated, and embedded in paraffin. Paraffin-embedded kidney tissues were sectioned into 4 μm thickness followed sequentially by dewaxing, hydration, and H&E staining. Glomerular retraction was observed using a light microscope under 10× magnification and quantified by counting the number of retracted glomeruli over the number of total glomeruli. Representative figures were obtained at 40×. Glomeruli with visible vascular pole and afferent and efferent arterioles were included in the analysis, while glomeruli with deformations in shape were excluded.

Proximal convoluted tubule (PCT) cross-sectional area (CSA), glomerular capillary area, and Bowman's capsule area were assessed using periodic acid–Schiff (PAS) staining. Briefly, kidney tissues were fixed with 4% formalin, dehydrated, and embedded in paraffin. Paraffin-embedded kidney tissues were sectioned into 4 μm thickness followed by dewaxing and hydration. The slides were stained with 0.5% PAS for 10 min, incubated with Schiff reagent for 20 min, and then washed for 5 min according to manufacturer's protocol (Periodic Acid Schiff Stain Kit, Mucin Stain, Abcam, ab150680). Slides were mounted and observed under light microscope at 40×. PCT cross sectional area, glomerular capillary area, and Bowman's capsule area were measured using ImageJ software (https://imagej.nih.gov/ij/). For glomerular capillary area and Bowman's capsule area analysis, glomeruli with visible vascular pole and afferent and efferent arterioles were included, whereas glomeruli with deformation in shape were excluded.

Total renal fibrosis was assessed using Masson's trichrome (MTC) staining. Briefly, kidney tissues were fixed with 4% formalin, dehydrated, and embedded in paraffin. Paraffin-embedded kidney tissues were sectioned into 4 μm thickness followed by dewaxing and hydration. Kidney tissues were then soaked in Bouin solution at 56°C for 1 h, washed, and rinsed in distilled water. Kidney sections were stained in hematoxylin for 10 min, washed, and incubated with Biebrich scarlet acid fuchsin. Finally, kidney tissues were washed again, differentiated in phosphomolybdic-phosphotungstic acid solution for 10 min, and stained with aniline blue solution for 5 min. Total renal fibrosis was observed under light microscopy at 10× magnification and measured using ImageJ software.

Protein extraction and Western blots

Snap-frozen kidneys were crushed under liquid nitrogen and homogenized using extraction buffer composed of 100 mM dithiothreitol, 1% sodium dodecyl sulfate (SDS), 0.9% NaCl, and 80 mM Tris hydrochloride (pH 6.8). Kidney tissues were then heated at 95°C for 10 min and left on a rocking shaker overnight at 4°C. Protein samples (150 μg) were loaded on to 15% gels for sodium dodecyl sulfate polyacrylamide gel electrophoresis (SDS-PAGE). Proteins were separated and transferred to nitrocellulose membranes. Membranes were blocked in 5% fat-free milk dissolved in TBS with 0.1% Tween 20 (TBST 0.1%) for 1 h at room temperature. Membranes were immunoblotted overnight at 4°C with antibodies against interleukin (IL)-1, IL-4, uncleaved caspase-3, and α-SMA (Table 1). TBS with 0.02% Tween 20 (TBST 0.02%) was used to wash the membranes (4 × 5 min). The membranes were incubated with 1:40,000 biotin-conjugated secondary antibody at room temperature for 1 h followed by four washes with TBST 0.02% for 5

Clinical Science (2023) **137** 47–63
https://doi.org/10.1042/CS20220513

Table 2 List of primers used for RT-qPCR analysis

Primer	Forward	Reverse
GAPDH	TGTGTCCGTGGATCTGA	TTGCTGTTGAAGTCGCAGGAG
NAMPT	ACCAGCGGGGAACTTTGTTA	ACATAACAACCCGGCCACAT
NMRK-1	CTTGAAGCTTGCTCTGCGAC	GTGTCGTCTTCCCTCCGTTT
PARP-1	ACACCACAAAACCTCAGCCA	ACAAACCACAAACAACCGGC

min each, then incubated with 1/200,000 HRP-conjugated streptavidin for 30 min. After washing with TBST 0.02% and finally TBS (2 × 5 min), bands were visualized using a Chemidoc MP imaging system (Bio-Rad) and ECL Chemiluminescence kit (Bio-Rad). To mitigate loading differences, protein expression levels were normalized to total protein per lane using Coomassie blue staining [24,25]. Total protein bands were obtained using the Chemidoc MP and analyzed via ImageJ software. A freshly prepared mild stripping buffer (200 mM glycine, 0.1% SDS, 1% v/v Tween 20, pH 2.2) was used for membrane stripping. Membranes were incubated 2 × 10 min with the buffer at room temperature, followed by 2 × 5 min washes with 0.02% TBST and then 2 × 5 min with TBS.

RNA extraction and real time-quantitative polymerase chain reaction

Snap-frozen kidney tissues were crushed under liquid nitrogen followed by total RNA extraction using TRIzol according to the manufacturer's instructions (Thermo Fisher Scientific, Grand Island, NY, U.S.A.). A NanoDrop ND-1000 was used to quantify RNA. Differences in mRNA expression levels were quantified using real-time q-PCR. Briefly, cDNA was synthesized from 1 μg RNA using the QuantiTect Reverse Transcription Kit (Qiagen), followed by real-time PCR in a CFX96 instrument (Bio-Rad, Germany). Samples were loaded in duplicate with 0.05 μl of the forward and reverse primers (Table 2) of the genes for the following: nicotinamide phosphoribosyltransferase (NAMPT), nicotinamide riboside kinase-1 (NMRK1), and poly (ADP-ribose) polymerase 1 (PARP-1) and mixed with SYBR® Green. Gene expression was normalized to glyceraldehyde-3-phosphate dehydrogenase (GAPDH). To check for non-specific amplification, no-template (water without DNA) was used. Normalized fold-expression relative to the control was calculated and plotted by Biorad CFX-manager to compare differential gene expression.

Total NAD extraction and quantification

Ten volumes (μl/mg) of buffered 75% ethanol and 25% HEPES (10 mM, pH 7.1) were used to extract 20 mg of kidney tissues. Extracts were diluted 1:20 in distilled water for a total minimum volume of 50 μl per dilution to reach a concentration within the standard curve. Afterward, 25 μl of NAD samples were loaded in a 96-well microtiter-plate in duplicate. Ten μl/well of reaction buffer (600 mM ethanol, 0.5 mM 3-(4.5dimethylthiazol-2-yl)-2.5-diphenyltetrazolium bromide [MTT]), 2 mM phenazine ethosulfate (PES), 120 mM bicine (pH 7.8) was added. Yeast alcohol dehydrogenase (Sigma-Aldrich A3263 > 300 units/mg) was then added to the NAD samples. The kinetics of the reaction (OD at 550 nm, every 30 s for 20 min) was examined on an LB 942 multimode reader and NAD was quantified using a linear regression curve equation method between NAD standard concentration and the slope of the regression line.

Statistical analysis

GraphPad Prism 9 software was used for statistical analysis. Results are expressed as fold change or mean ± standard error of the mean (SEM). Statistical comparisons were performed using two-way ANOVA and a Tukey's or Sidak's multiple comparisons test, or by unpaired *t*-test or Mann–Whitney test. For the two-way ANOVA, capillary area, glomerular retraction, and PCT-CSA were significant for interaction (MI × sex) and sex; ejection fraction (EF), IL-1β, IL-4, NAD, creatinine clearance, glomerular ROS, and urine output were significant for MI only; all other parameters were significant for interaction, MI, and sex. A P-value of <0.05 was considered significant.

Results

OVX enhanced the decrease with MI in ejection fraction

Figure 1A shows a comparable decrease in EF in MI mice of both sexes compared with their respective controls ($P<0.05$). As for the impact of OVX on FMI mice, Figure 1B shows an exacerbated decrease in EF in FMIOVX mice compared with the FMI group ($P<0.05$).

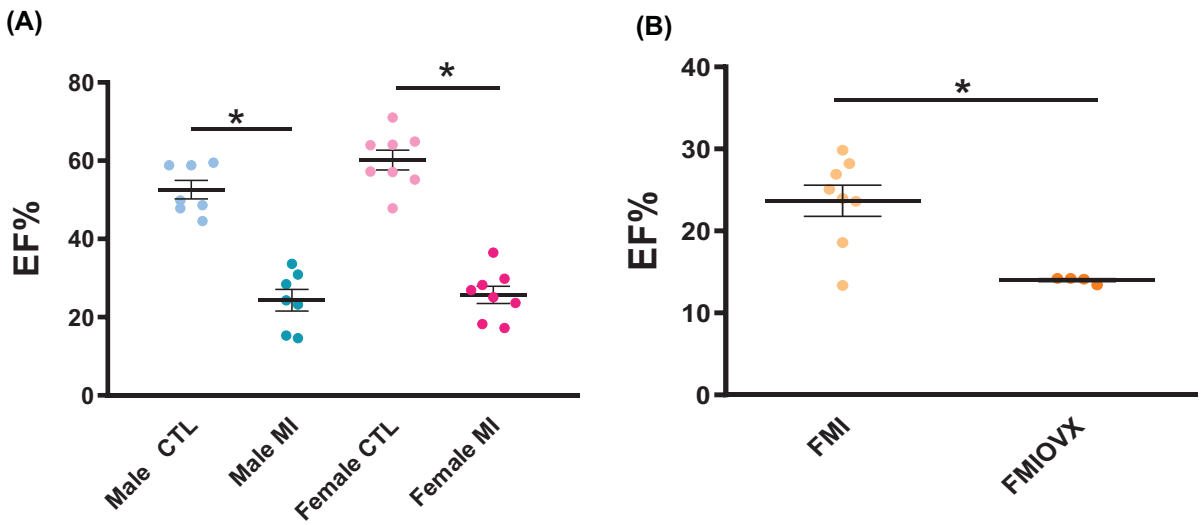

Figure 1. Comparison of EF between MMI and FMI mice, and between FMI and FMIOVX

EF markedly decreased in MI mice of both sexes compared with their relative control groups (**A**). EF significantly decreased in FMIOVX mice compared with the FMI group (**B**). Data were analyzed for MMI and FMI using two-way ANOVA, and for FMI and FMIOVX using unpaired *t*-test. All bars represent mean ± SEM (*$P<0.05$; $n=4$–13); MI, myocardial infarction; OVX, ovariectomy.

OVX did not eliminate the female-sex protection of glomerular morphology but did cause swelling of proximal convoluted tubules with MI

Figure 2A–C shows an increase in glomerular retraction and in the Bowman's capsule area, and a decrease in glomerular capillary area, in MI male mice compared with their control group and female mice ($P<0.05$). OVX did not have any impact on kidney morphology (glomerular retraction, Bowman's capsule area, and glomerular capillary area) in FMI mice (Figure 2D–F).

Figure 3A shows enhanced proximal convoluted tubule cross-sectional area (PCT-CSA) in MI male mice compared with their controls and female mice ($P<0.05$). Females did not show a significant increase with MI; however, with OVX there was a significant increase in PCT-CSA in FMIOVX mice compared with the FMI group ($P<0.05$) (Figure 3B).

OVX eliminated the attenuated increase in inflammatory IL-1β with MI but did not alter caspase-3 or anti-inflammatory IL-4 levels

We assessed the effect post-MI of OVX on differences between males and females in pro- and anti-inflammatory cytokines and caspase-3, which has a role in apoptosis by both the extrinsic and intrinsic pathways. Figure 4A–C reveals increased IL-1β, uncleaved caspase-3, and IL-4 protein levels in kidneys of male mice with MI compared with controls ($P<0.05$). Female mice, however, show no changes in uncleaved caspase-3 protein levels in the kidneys post-MI. Female mice showed an increase with MI in IL-1β and IL-4 protein levels, but this did not reach significance. As for the impact of OVX, Figure 4D shows a significant increase in IL-1β protein levels in the kidneys of FMIOVX mice compared with the FMI group ($P<0.05$), whereas no significant change in caspase-3 nor IL-4 protein levels in the kidneys of FMIOVX mice compared with the FMI group was observed (Figure 4E,F). The effect of MI and OVX on systemic inflammation was assessed in terms of plasma TNF-α levels, which were under the detection limit (<5 pg/ml) in all groups.

OVX had mixed effects on female-related increases in NAD^+ generating enzymes with MI but did not protect NAD levels

We next assessed the effect of OVX on sex-based differences in NAD^+ biosynthetic enzymes of the kidney after MI. NAD^+ is a major coenzyme for glycolysis and mitochondrial oxidative phosphorylation [26]. Furthermore, NAD^+ is an essential substrate of crucial enzymes involved in regulating metabolism, cellular repair, and maintaining cellular

Clinical Science (2023) **137** 47–63
https://doi.org/10.1042/CS20220513

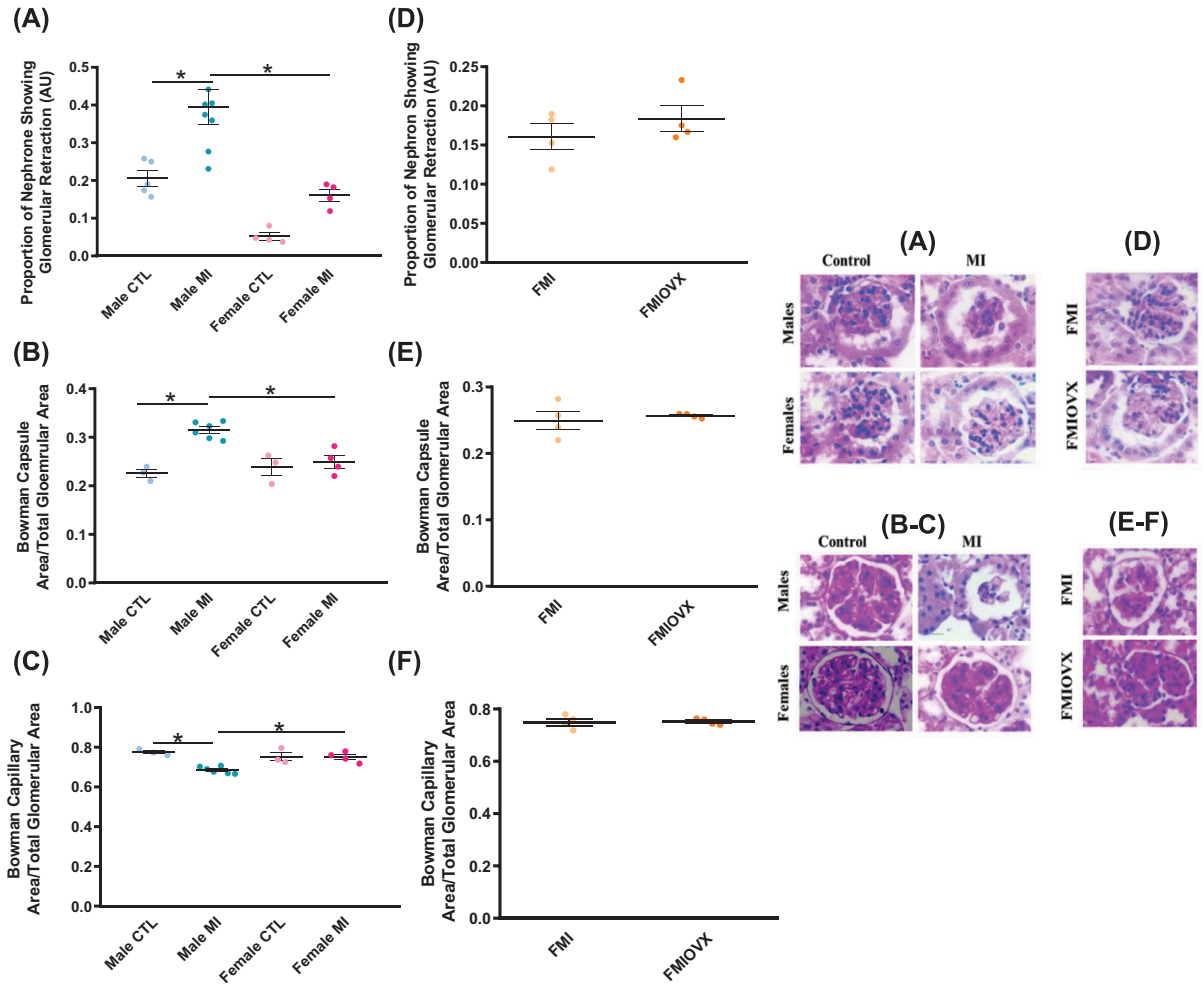

Figure 2. Glomerular alterations in MMI, FMI, and FMIOVX mice

Glomerular retraction and the Bowman's capsule area markedly increased in MI males, but not in MI females (**A,B**). Glomerular capillary area decreased in MI male mice but not MI females (**C**). There was no change in glomerular retraction, Bowman's capsule area, and glomerular capillary in FMIOVX mice compared with FMI mice (**D–F**). Representative image of each stained group is shown. Data were analyzed for MMI and FMI using two-way ANOVA, and for FMI and FMIOVX by unpaired *t*-test. All bars represent mean ± SEM (*$P<0.05$, $n=3–7$).

homeostasis [27]. Figure 5A,B show a significant increase in NAMPT and NMRK-1 mRNA expression levels in the kidneys of MI female mice compared with their controls ($P<0.05$). Male mice, however, showed no change in renal NAMPT and NMRK-1 mRNA expression levels post-MI ($P<0.05$). A significant difference between male and female MI mice was observed. Figure 5C shows a comparable decrease in total NAD levels in the kidneys of mice of both sexes after MI ($P<0.05$). As for the impact of OVX, Figure 5D shows a significant decrease in NAMPT mRNA expression levels in the kidneys of FMIOVX mice compared with the FMI group ($P<0.05$). In contrast, NMRK-1 mRNA expression levels markedly increased in the kidneys of FMIOVX mice compared with the FMI group ($P<0.05$) (Figure 5E). However, Figure 5F shows no significant change in total NAD levels in the kidneys of FMIOVX mice compared with the FMI group.

PARP-1 can lead to NAD depletion. Figure 6A shows a marked increase in PARP-1 mRNA expression levels in kidneys of males with MI ($P<0.05$). Female mice, however, show no change in PARP-1 mRNA expression levels in the kidneys post-MI. There was no significant change in PARP-1 mRNA expression levels in the kidneys of FMIOVX mice (Figure 6B).

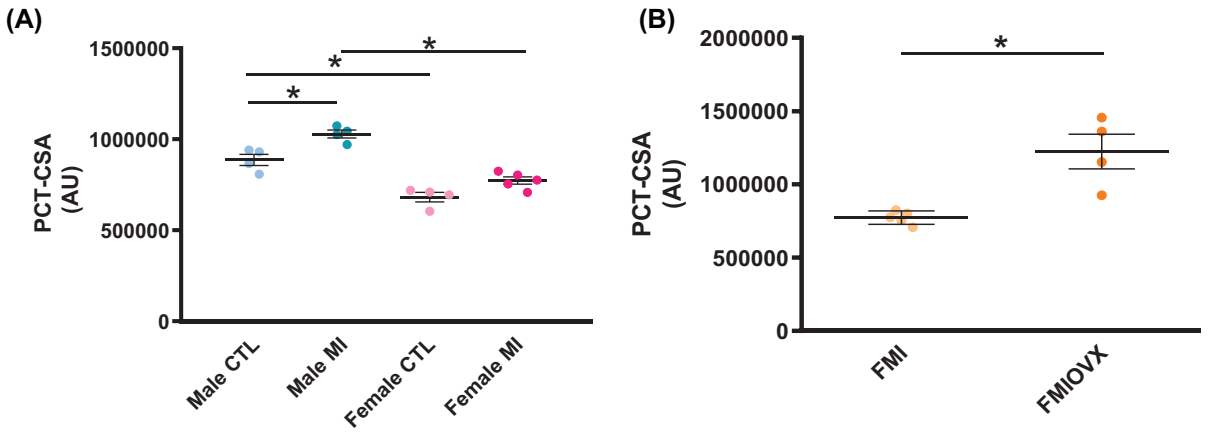

Figure 3. PCT-CSA comparison among MMI, FMI, and FMIOVX mice

PCT-CSA significantly increased with MI in male mice compared with females (**A**). PCT-CSA substantially increased in FMIOVX mice compared with the FMI group (**B**). Data were analyzed for MMI and FMI using two-way ANOVA, and for FMI and FMIOVX by unpaired *t*-test. All bars represent mean ± SEM (*$P<0.05$, $n=3–7$).

Females have lower kidney fibrosis after MI regardless of OVX

The α-SMA protein is a marker of myofibroblasts and fibrosis. Figure 7A shows a significant increase in α-SMA protein levels in the kidneys of male mice following MI ($P<0.05$). Female mice, however, had no significant change in α-SMA protein levels in the kidneys post-MI. A significant difference between MI males and MI females was observed. As for the impact of OVX, Figure 7B shows no significant change in α-SMA protein levels in the kidneys of FMIOVX mice compared with the FMI group. Our data were further supported by IF showing an accumulation of α-SMA in the peritubular space of the kidneys of MI male mice only (Supplementary Figure S2).

Figure 8A shows a significant increase in total renal fibrosis in male mice with MI compared with their control group and female MI mice ($P<0.05$). No significant difference between control male and female mice was observed. As for the impact of OVX, Figure 8B shows a modest increase in total renal fibrosis in FMIOVX mice compared with the FMI group ($P<0.05$).

Ovariectomy exacerbates kidney damage following MI

Figure 9A shows a comparable decrease in creatinine clearance (CrCl) in both sexes post-MI ($P<0.05$). Whereas as shown in Figure 9B, there was a marked decrease in urine output in male mice post-MI ($P<0.05$), there was no significant change in urine output in MI female mice compared with their controls. No significant difference in CrCl and urine output between control male and female mice was observed. Figure 9C reveals no significant change in urine protein concentration in either sex post-MI, although a significant difference in urine protein concentration was observed between male and female mice regardless of MI ($P<0.05$). As for the impact of OVX, Figure 9D,E shows a marked decrease in CrCl and urine output in FMIOVX mice compared with the FMI group ($P<0.05$). No significant change in protein concentration of urine was observed in FMIOVX mice compared with the FMI group (Figure 9F).

Discussion

Accumulating experimental and clinical studies report a positive correlation between acute cardiac injury and kidney disease development and progression [28–30]. In the present study, we affirmed that male mice are in general more susceptible to alterations in renal function and structure following MI than age-matched premenopausal female mice (Table 3). Comparable sex differences in some of these parameters were reported previously in a study examining the consequences of tobacco smoking [31]. Here, we extend those findings and address the potential contribution of estrogen to this protection by performing ovariectomy (OVX). Notably, a number of parameters related to kidney structure and function were not affected by ovariectomy. These include changes strongly observed in males with MI, such as increased glomerular retraction and Bowman's capsule area, decreased glomerular capillary area, and increased renal IL-4, PARP-1, and α-SMA expression. Total NAD was depressed by MI in both sexes and was not further

Clinical Science (2023) **137** 47–63
https://doi.org/10.1042/CS20220513

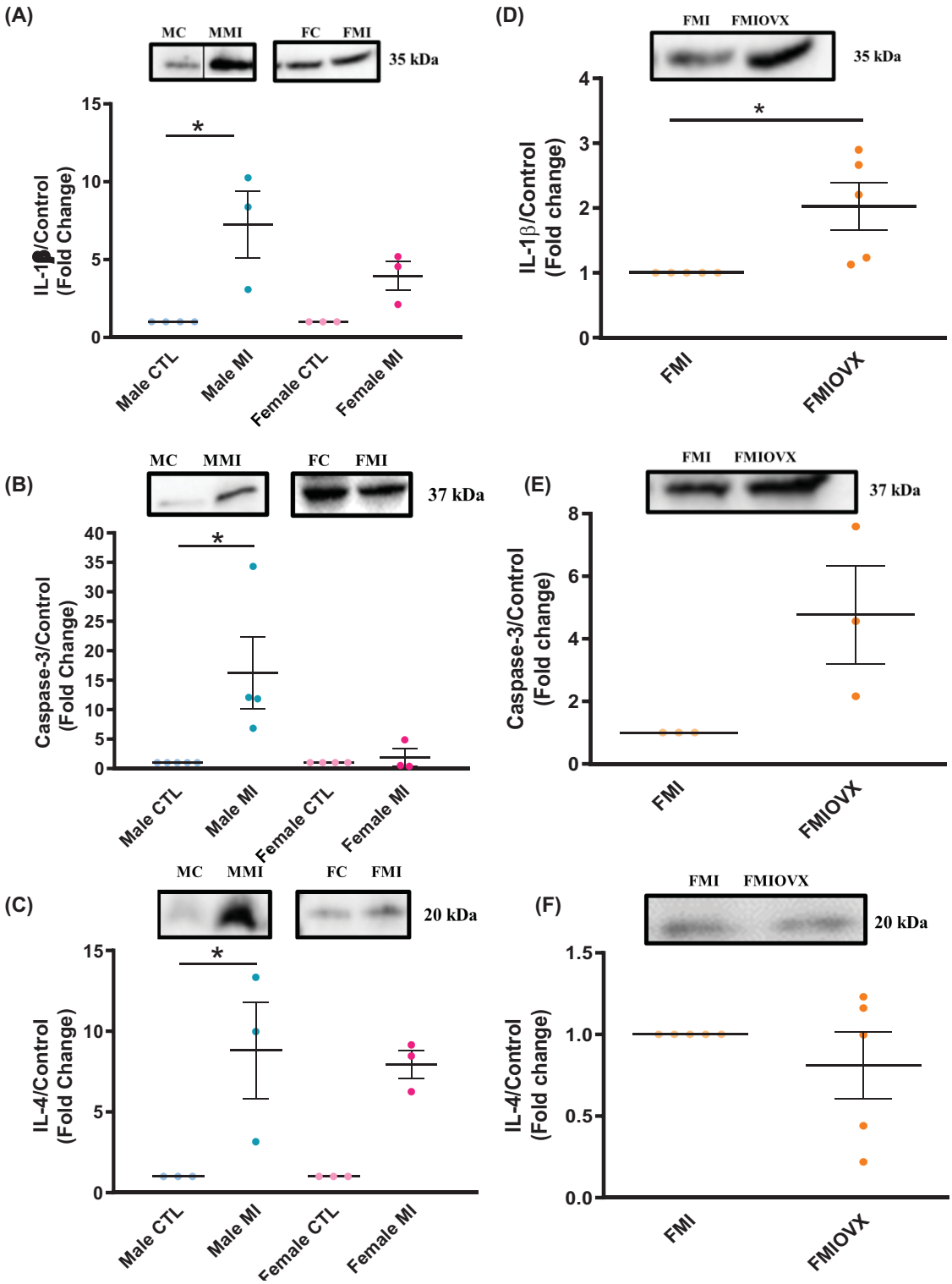

Figure 4. Renal cytokine and caspase-3 comparisons in MMI, FMI, and FMIOVX mice

IL-1β protein levels significantly increased in the kidneys of MI male mice compared with their controls (**A**). Uncleaved caspase-3 markedly increased in the kidneys of MI male mice but not in females (**B**). IL-4 protein levels substantially increased in the kidneys of MI male mice compared with their controls groups (**C**). IL-1β but not caspase-3 and IL-4 substantially increased in FMIOVX mice compared with the FMI group (**D–F**). Representative image of each blot is shown. IL-1β and caspase-3 protein levels were normalized to total protein (Supplementary Figure S1). Data were analyzed for MMI and FMI using two-way ANOVA, and for FMI and FMIOVX using unpaired *t*-test. All bars represent mean ± SEM (*$P<0.05$, $n=3–5$).

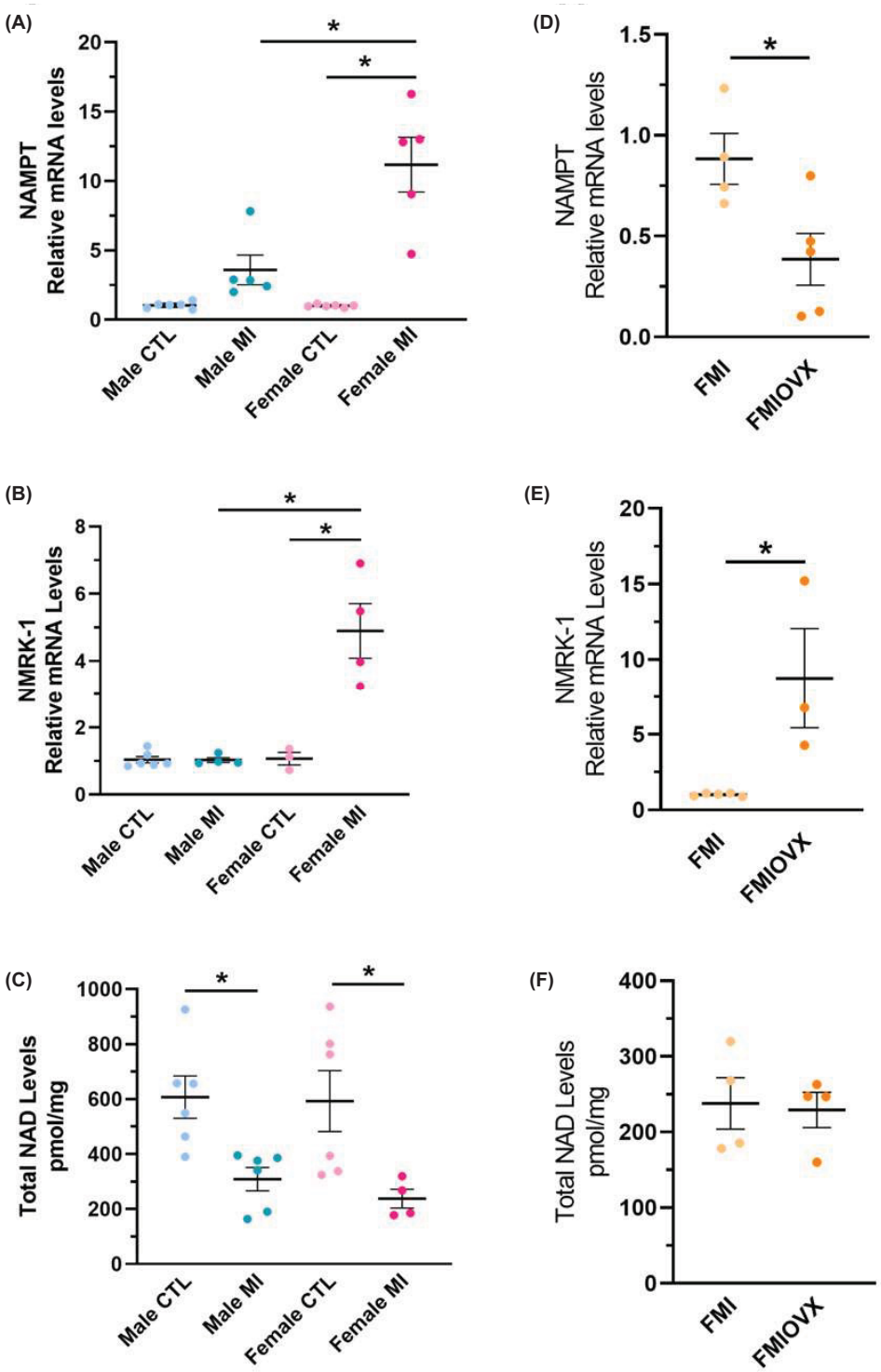

Figure 5. Comparison of NAD$^+$ biosynthetic enzymes and total renal NAD levels between MMI and FMI mice, and between FMI and FMIOVX

NAMPT and NMRK-1 mRNA expression levels significantly increased in the kidneys of MI female mice compared with the relative male group (**A,B**). Total renal NAD levels decreased in both sexes with MI (**C**). NAMPT mRNA expression levels decreased in the kidneys of FMIOVX mice compared with the FMI group (**D**), whereas NMRK-1 mRNA expression levels significantly increased in the kidneys of FMIOVX mice compared with the FMI group (**E**). No significant change in total NAD levels in the kidneys of FMIOVX mice compared with the FMI group was observed (**F**). Data were analyzed for MMI and FMI using two-way ANOVA, and for FMI and FMIOVX using unpaired *t*-test. All bars represent mean ± SEM (*$P<0.05$).

Clinical Science (2023) **137** 47–63
https://doi.org/10.1042/CS20220513

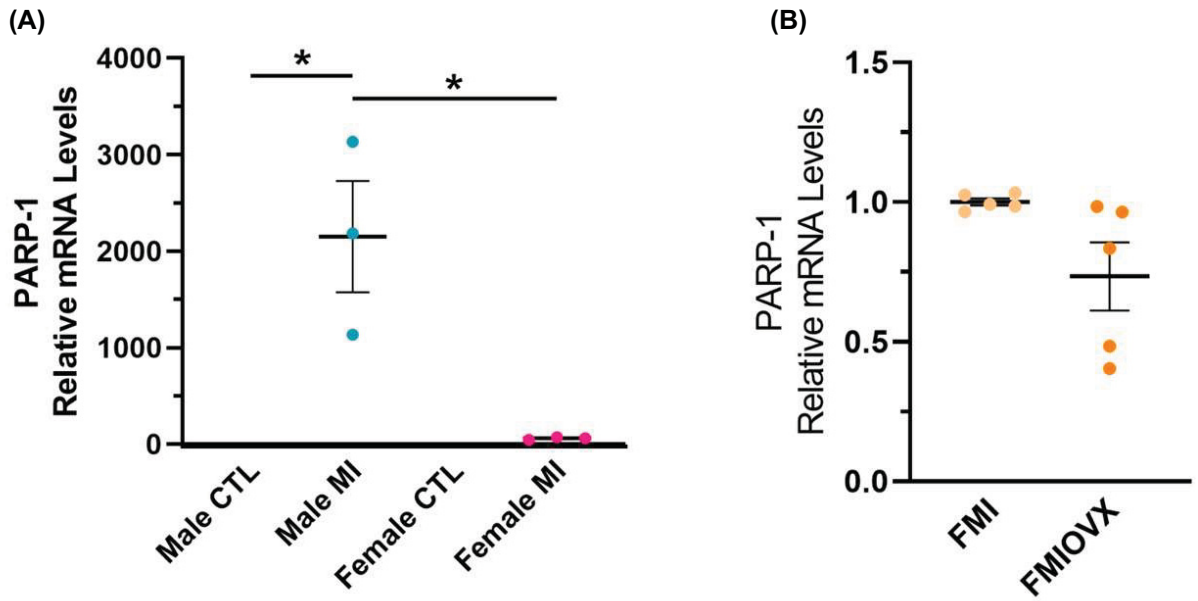

Figure 6. The effects of MI and OVX on PARP-1 in the kidney

PARP-1 mRNA expression levels significantly increased in the kidneys of male mice with MI compared with females (**A**). No significant increase in PARP-1 mRNA expression levels was observed in the kidneys of FMIOVX mice compared with the FMI group (**B**). Data were analyzed for MMI and FMI using two-way ANOVA, and for FMI and FMIOVX using unpaired *t*-test. All bars represent mean ± SEM (*$P<0.05$).

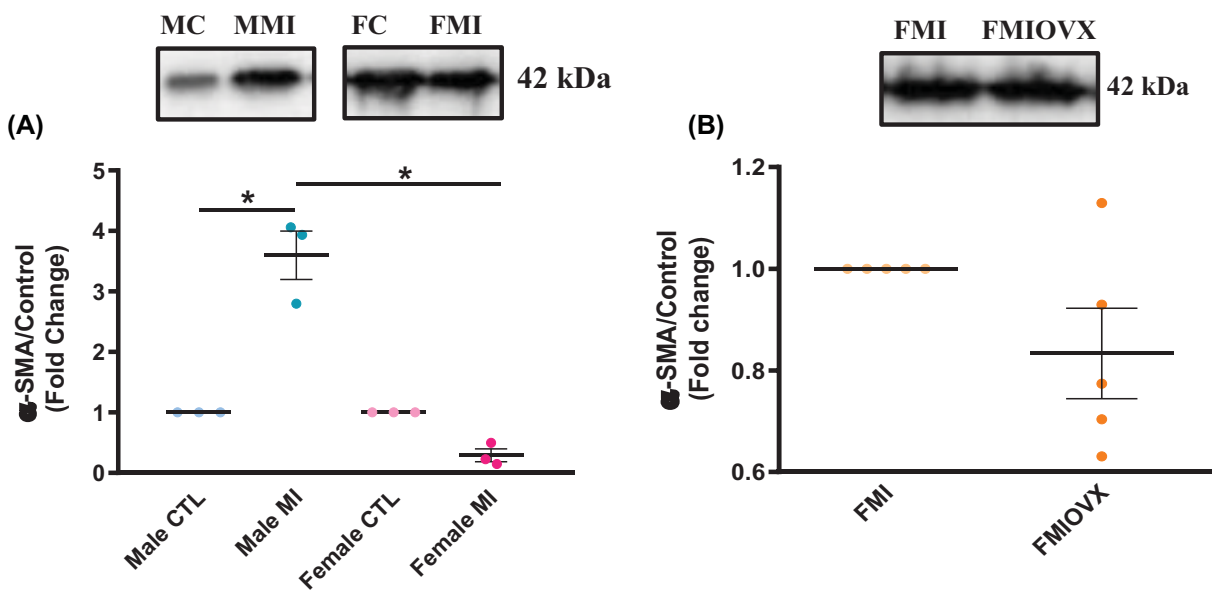

Figure 7. The effects of MI and OVX on α-SMA protein levels

α-SMA protein significantly increased in the kidneys of MI male unlike females (**A**). No significant change in α-SMA protein levels in the kidneys of FMIOVX mice compared with the FMI group was observed (**B**). α-SMA protein levels were normalized to total protein (Supplementary Figure S3). Data were analyzed for MMI and FMI using two-way ANOVA, and for FMI and FMIOVX using unpaired *t*-test. All bars represent mean ± SEM (*$P<0.05$, $n=3–4$).

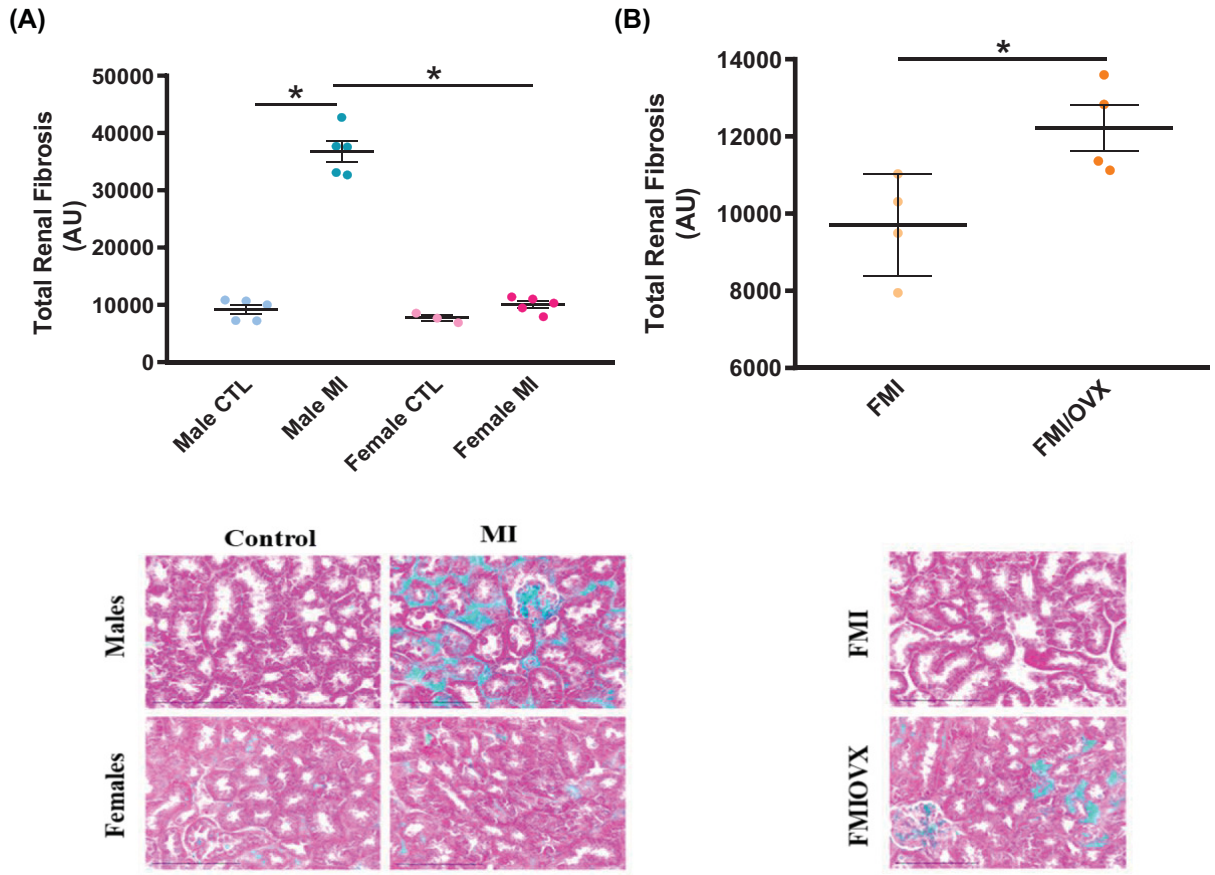

Figure 8. The effects of MI and OVX on total renal fibrosis

Total renal fibrosis significantly increased in male mice with MI compared with females (**A**). Total renal fibrosis increased in FMIOVX mice compared with the FMI group (**B**). Representative image of each MTC stained group is shown. Data were analyzed for MMI and FMI using two-way ANOVA, and for FMI and FMIOVX using unpaired *t*-test. All bars represent mean ± SEM (*$P<0.05$, $n=3–7$).

Table 3 Key findings

Parameter	MMI	FMI	FMIOVX vs. FMI
Glomerular retraction	↑↑	~↑	nc
Bowman's capsule area	↑	nc	nc
Glomerular capillary area	↓	nc	nc
PCT-CSA	↑	nc	↑
IL-1β	↑↑	~↑	↑
Caspase-3	↑↑	nc	~↑
IL-4	↑↑	~↑	nc
NAMPT	~↑	↑↑	↓
NMRK-1	nc	↑↑	↑↑
Total NAD	↓↓	↓↓	nc
PARP-1	↑↑	nc	~↓
α-SMA	↑↑	nc	nc
Renal fibrosis	↑↑	nc	↑
Creatinine clearance	↓↓	↓↓	↓↓
Urine output	↓	nc	↓
Urine protein	nc	nc	~↓

Abbreviations: ~, trend; nc, no change; PCT-CSA, proximal convoluted tubule cross-sectional area.

Clinical Science (2023) **137** 47–63
https://doi.org/10.1042/CS20220513

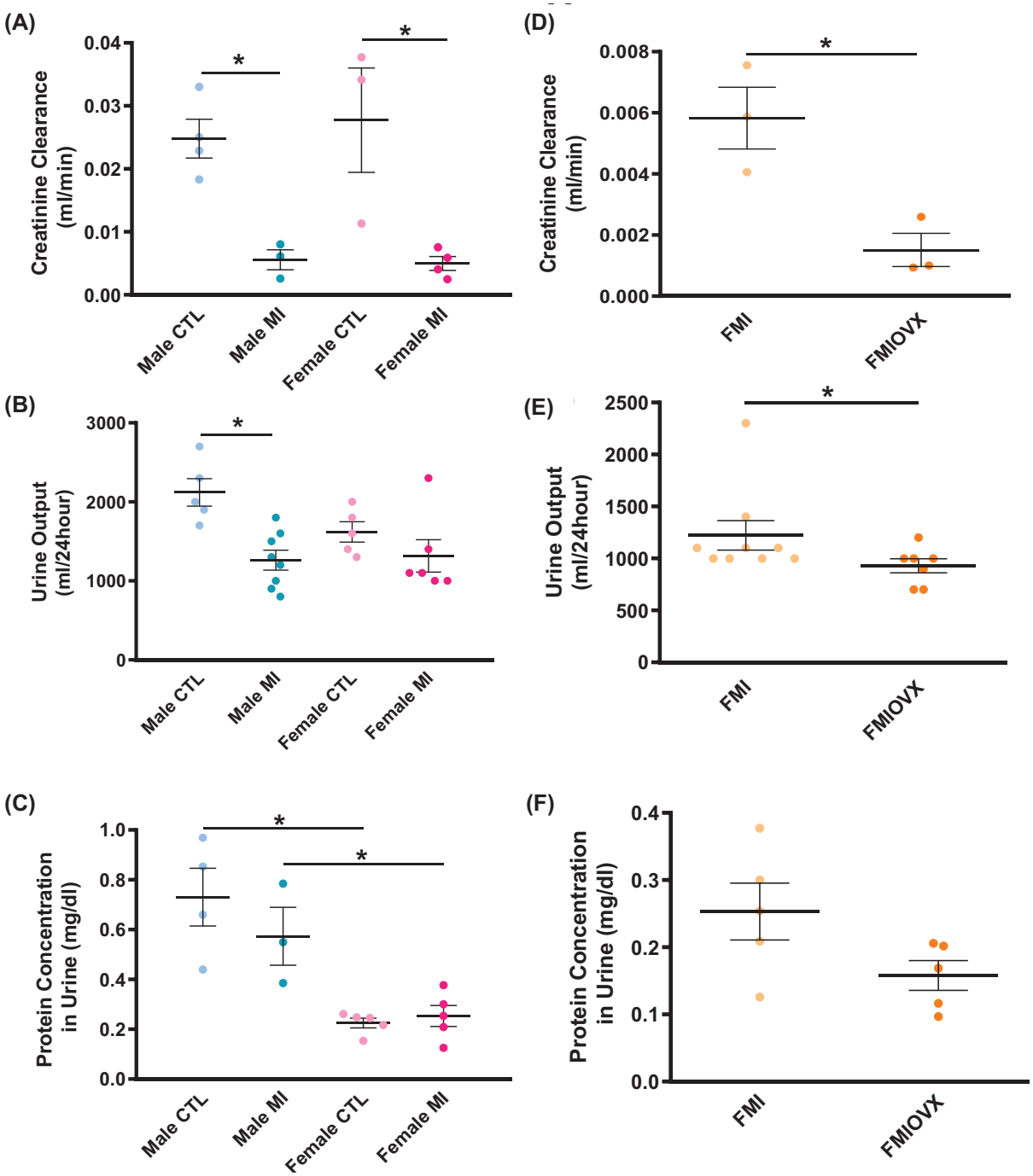

Figure 9. Effects of MI and OVX on CrCl, urine output, and urine protein concentration

CrCl was decreased with MI mice in both sexes (**A**). Urine output was markedly decreased in MI male mice compared with controls (**B**). No change in urine protein concentration with MI mice of both sexes was observed (**C**). CrCl and urine output decreased in FMIOVX mice compared with the FMI group (**D,E**), whereas no change was observed in urine protein concentration in FMIVX mice compared with the FMI group (**F**). Data were analyzed for MMI and FMI using two-way ANOVA, and for FMI and FMIOVX using unpaired *t*-test. All bars represent mean ± SEM (*$P<0.05$, $n=3–9$).

affected by OVX. However, levels of NAD generating enzymes NAMPT and NMRK-1 were increased in females with MI (but not males), and OVX attenuated and enhanced these changes, respectively. A good number of parameters were indeed changed in a more male-like direction by OVX, including increased PCT-CSA, increased renal IL-1β, caspase-3, and fibrosis, and decreased creatinine clearance, and urine output. OVX also tended to decrease urine protein, which otherwise was not seen in females or in males. These findings suggest that while estrogen provides some protection to the kidney after MI, other factors come into play as well, such as pre-exiting structural differences. In addition, a further decrease in EF after MI with OVX may negatively impact on renal function and structure. In this regard, Cavasin et al. also reported that OVX decreased EF in mice post-MI, leading to worsen cardiac function and aggravated LV adverse remodeling [32]. The further decrease in EF seen with OVX might be attributed to the harmful effects of increased sympathetic drive on the injured heart in female mice [33–35]. Moreover, increased sympathetic drive may have had direct harmful effects on the kidney, so that any harmful effects of OVX may reflect an indirect effect of estrogen loss.

Hemodynamic analysis showed a marked decrease in EF, indicating cardiac dysfunction and enhanced adverse LV remodeling, 7 days post-MI occurring equally in both sexes. The absence of systemic inflammation as observed with undetectable plasma TNF-α levels in mice of both genders, not only correlates with previous studies [36,37] but also rules out any potential correlation between kidney damage and persistent systemic inflammation at 7 days post-MI. With the absence of any pronounced or evident differences between male and premenopausal female mice in systemic hemodynamics and inflammation at 7 days post-MI, the observed sexual dimorphism in MI-induced kidney damage was tracked down to kidney molecular, metabolic, structural, and functional levels.

Our data indicated pronounced renal structural alterations in MI mice of both sexes but to a greater extent in males. For instance, glomerular retraction, glomerular capillary area, Bowman's capsule area, PCT-CSA, and renal fibrosis significantly increased in MI male mice compared with their female counterparts. These outcomes are in accordance with non-sex-based studies. For instance, it has been reported that PCT-CSA was markedly enhanced in male mice 7 days following MI [38]. Additionally, Sasak et al. showed that changed glomerular capillary area to the Bowman's capsule area is tightly linked to the initial phase of glomerular injury [39]. In agreement, Munshi et al. indicated that glomerular retraction is the histological hallmark of ischemic glomerular damage [40]. Similarly, Lekawanvijit et al. demonstrated that male Sprague–Dawley rats developed renal interstitial fibrosis post-MI, resulting therefore in enhanced kidney dysfunction [41].

The proinflammatory cytokine IL-1β and proapoptotic marker caspase-3 significantly increased in MI male mice, while remaining unchanged in female mice post-MI. Of note, we did not see an increase in cleaved caspase-3 in MI male mice probably because of timing (data not shown); we postulate that the increase in uncleaved caspase 3 represents a compensatory response. Moreover, increased caspase 3 and IL-1β may reflect aspects of pyroptosis-related inflammasome activity in male MI mice [42].

IL-1β has been implicated in exacerbated kidney pathology [43,44]. Additionally, it has been shown that caspase-3, an executioner caspase implicated in DNA fragmentation, induces kidney apoptosis and fibrosis [45]. A marked increase in IL-4 was observed in MI male mice, only. The role of IL-4 in the setting of kidney diseases including AKI is still controversial. For instance, it has been demonstrated that IL-4 stimulates the polarization of the proinflammatory M1 phenotype into the anti-inflammatory M2 phenotype, thereby decreasing tubular injury [46]. In contrast, a study performed by Kim et al. indicated that overexpression of IL-4 enhanced glomerular injury and kidney damage [47].

Inflammation is known to play a central role in the development of fibrosis and cell death, key elements contributing to kidney disease development [48,49]. Unlike MI females, α-SMA significantly increased in MI male mice. Multiple studies have reported that α-SMA is the hallmark of extracellular matrix deposition, resulting in enhanced fibrosis [50,51].

NAD^+ salvage biosynthetic, dependent, consuming enzymes, and total NAD levels were assessed as markers of potential mitochondrial dysfunction and necrotic cell death. Both NAMPT and NMRK-1 levels, NAD^+ biosynthetic salvage enzymes, substantially increased in MI female mice compared with the male counterparts. NAMPT and NMRK-1 are involved in converting nicotinamide (NAM) and nicotinamide riboside (NR) respectively, to nicotinamide mononucleotide (NMN) and subsequently NAD^+ [52,53]. Unlike in females, PARP-1, an NAD^+ consuming enzyme, markedly increased in male mice with MI. It has been reported that overactivation of PARP-1 leads to NAD^+ depletion, subsequently enhanced energy loss and cell death [54]. Total renal NAD levels, however, decreased in MI mice of both sexes to the same extent. Previous evidence reported a positive correlation between altered NAD^+ biosynthetic and dependent enzymes and exacerbated NAD^+ depletion [55–57]. For instance, it has been demonstrated that enhanced NAMPT levels, the main NAD^+ biosynthetic enzyme, results in increased NAD^+ levels and enhanced cellular function [56,58]. Thus, a more extensive time course is needed to establish whether NAD levels recovered (more so) in female versus male mice after MI.

Clinical Science (2023) **137** 47–63
https://doi.org/10.1042/CS20220513

Our findings indicate enhanced renal structural alterations including increased PCT-CSA and interstitial fibrosis with MI following OVX. Notably, there were no changes with OVX in the lack of an effect in females with MI on glomerular retraction, glomerular capillary area, and Bowman's capsule area. Multiple studies are in accordance with our outcomes [22,59,60]. NAMPT markedly decreased in MI female mice following OVX, whereas NMRK-1 substantially increased, although total NAD levels were still depressed. Annie et al. reported that administration of estrogen to ovariectomized mice led to a boost in NAMPT level in mouse uterus [61].

The observed MI-induced structural and molecular alterations in the kidneys may contribute to deterioration in kidney function. Both sexes experienced a comparable decrease in CrCl 7 days post-MI, while urine output markedly decreased in MI male mice only. A pronounced decline in CrCl and urine output was also seen in MI female mice following OVX. CrCl reflects glomerular filtration rate (GFR) [62,63], indicating a potential decrease in GFR. Decreased urine output is a key determinant of the severity of AKI [64]. Proteinuria was also measured, showing no significant change in both sexes post-MI, a finding consistent with a previous study reporting that proteinuria is a pathogenic mechanism of chronic kidney disease and end-stage renal failure [65]. Our findings would indicate an early stage of decreased GFR without a loss of glomerular barrier function. Of note, a number of studies have demonstrated that CKD may develop in patients without proteinuria [66]. A limitation of our study is that we only used functional and damage biomarkers to assess AKI. Future studies will be done to measure novel serum and urinary proteins that have been identified as biomarkers of AKI.

Conclusion and future direction

The present study shows both sexes are prone to develop kidney damage post-MI, with premenopausal female mice being more protected against certain aspects of MI-induced kidney injury at least during the first 7 days post-MI. OVX worsens kidney dysfunction in female mice following MI, indicating a renal protective effect of ovarian estrogen. Exploration of the factors that might contribute to AKI with MI need to be better defined, such as those released from the injured heart (e.g., exosomes), activated immune cells, and stimulation of the sympathetic and renin–angiotensin–aldosterone systems. Hypoperfusion with oxygen deprivation and build-up of metabolic waste may play a role as well. Future experiments aimed at highlighting the effect of an aromatase inhibitor on MI-induced kidney damage in the FMIOVX group to decrease extra-gonadal estrogen synthesis is warranted. Additionally, characterizing the role of testosterone in the observed kidney injury in male mice post-MI by castration is needed.

Clinical perspectives

- MI is associated with elevated risk of AKI, through the cardiorenal interrelationship. Preclinical investigations and clinical studies showed that females are less prone to develop AKI following CVDs.
- Using a mouse model of MI-induced AKI, our data show that both male and premenopausal female mice experienced kidney deterioration at molecular, structural, and functional levels, with males being more affected. Ovariectomy negatively altered the observed kidney protection in females post-MI.
- The identification of sex-dependent molecular pathways involved in MI-mediated AKI renders promising targets to attenuate kidney injury post-MI.

Data Availability

The data that support the findings of this study are available from the corresponding author upon reasonable request.

Competing Interests

The authors declare that there are no competing interests associated with the manuscript.

Funding

This work was supported by grants from the American University of Beirut Faculty of Medicine [grant numbers MPP – 320145/320095 and URB – 103949]; Centre National de la Recherche Scientifique (CNRS) [grant number 103507/103487/103941/103944]; and Collaborative Research Stimulus [grant number 103556 (to F.A.Z.)].

CRediT Author Contribution

Nada J. Habeichi: Conceptualization, Resources, Data curation, Software, Formal analysis, Supervision, Validation, Investigation, Visualization, Methodology, Writing—original draft, Project administration, Writing—review & editing. **Rana Ghali:** Conceptualization, Data curation, Software, Formal analysis, Supervision, Validation, Methodology, Project administration. **Ali Mroueh:** Data curation, Software, Supervision, Validation, Investigation, Methodology. **Abdullah Kaplan:** Conceptualization, Formal analysis, Validation, Visualization, Methodology. **Cynthia Tannous:** Data curation, Formal analysis, Validation. **Abdo Jurjus:** Formal analysis, Methodology. **Ghadir Amin:** Data curation, Supervision, Writing—review & editing. **Mathias Mericskay:** Conceptualization, Software, Formal analysis, Supervision, Validation, Visualization, Project administration, Writing—review & editing. **George W. Booz:** Conceptualization, Formal analysis, Validation, Visualization, Writing—original draft, Project administration, Writing—review & editing. **Ahmed El-Yazbi:** Conceptualization, Resources, Data curation, Software, Formal analysis, Supervision, Validation, Methodology, Writing—original draft, Project administration. **Fouad A. Zouein:** Conceptualization, Supervision, Funding acquisition, Methodology, Project administration, Writing—review & editing.

Acknowledgements

We would like to thank Dr Hana Itani for her generous support by providing us with metabolic cages. GWB acknowledges the support of the Pharmacology Clinical Research Core of the University of Mississippi Medical Center.

Abbreviations

CrCl, creatinine clearance; CRS, cardiorenal syndrome; CVD, cardiovascular disease; EF, ejection fraction; GFR, glomerular filtration rate; MI, myocardial infarction; NAMPT, nicotinamide phosphoribosyltransferase; NMRK1, nicotinamide riboside kinase-1; OVX, ovariectomy; PARP-1, poly (ADP-ribose) polymerase 1; PCT-CSA, proximal convoluted tubule cross-sectional area.

References

1 Benjamin, E.J., Muntner, P., Alonso, A., Bittencourt, M.S., Callaway, C.W., Carson, A.P. et al. (2019) Heart Disease and Stroke Statistics-2019 Update: a report from the American Heart Association. *Circulation* **139**, e56–e528, https://doi.org/10.1161/CIR.0000000000000659
2 Bots, S.H., Peters, S.A. and Woodward, M. (2017) Sex differences in coronary heart disease and stroke mortality: a global assessment of the effect of ageing between 1980 and 2010. *BMJ Global Health* **2**, e000298, https://doi.org/10.1136/bmjgh-2017-000298
3 Bavry, A.A. and Limacher, M.C. (2014) Prevention of cardiovascular disease in women. *Seminars in Reproductive Medicine*, pp. 447–453, Thieme Medical Publishers
4 Kaplan, A., Abidi, E., Ghali, R., Booz, G.W., Kobeissy, F. and Zouein, F.A. (2017) Functional, cellular, and molecular remodeling of the heart under influence of oxidative cigarette tobacco smoke. *Oxid. Med. Cell Longev.* **2017**, 3759186, https://doi.org/10.1155/2017/3759186
5 Benjamin, E.J., Blaha, M.J., Chiuve, S.E., Cushman, M., Das, S.R., Deo, R. et al. (2017) Heart Disease and Stroke Statistics-2017 Update: a report from the American Heart Association. *Circulation* **135**, e146–e603, https://doi.org/10.1161/CIR.0000000000000485
6 Dunlay, S.M. and Roger, V.L. (2012) Gender differences in the pathophysiology, clinical presentation, and outcomes of ischemic heart failure. *Curr. Heart Fail. Rep.* **9**, 267–276, https://doi.org/10.1007/s11897-012-0107-7
7 Deedwania, P.C. (2000) Silent myocardial ischaemia in the elderly. *Drugs Aging* **16**, 381–389, https://doi.org/10.2165/00002512-200016050-00007
8 Reckelhoff, J.F. and Samson, W.K. (2015) *Sex and gender differences in cardiovascular, renal and metabolic diseases*, American Physiological Society, Bethesda, MD
9 Lerner, D.J. and Kannel, W.B. (1986) Patterns of coronary heart disease morbidity and mortality in the sexes: a 26-year follow-up of the Framingham population. *Am. Heart J.* **111**, 383–390, https://doi.org/10.1016/0002-8703(86)90155-9
10 Smith, G.L., Lichtman, J.H., Bracken, M.B., Shlipak, M.G., Phillips, C.O., DiCapua, P. et al. (2006) Renal impairment and outcomes in heart failure: systematic review and meta-analysis. *J. Am. Coll. Cardiol.* **47**, 1987–1996, https://doi.org/10.1016/j.jacc.2005.11.084
11 Heywood, J.T., Fonarow, G.C., Costanzo, M.R., Mathur, V.S., Wigneswaran, J.R., Wynne, J. et al. (2007) High prevalence of renal dysfunction and its impact on outcome in 118,465 patients hospitalized with acute decompensated heart failure: a report from the ADHERE database. *J. Card. Fail.* **13**, 422–430, https://doi.org/10.1016/j.cardfail.2007.03.011
12 Adams, Jr, K.F., Fonarow, G.C., Emerman, C.L., LeJemtel, T.H., Costanzo, M.R., Abraham, W.T. et al. (2005) Characteristics and outcomes of patients hospitalized for heart failure in the United States: rationale, design, and preliminary observations from the first 100,000 cases in the Acute Decompensated Heart Failure National Registry (ADHERE). *Am. Heart J.* **149**, 209–216, https://doi.org/10.1016/j.ahj.2004.08.005
13 Triposkiadis, F., Giamouzis, G., Parissis, J., Starling, R.C., Boudoulas, H., Skoularigis, J. et al. (2016) Reframing the association and significance of co-morbidities in heart failure. *Eur. J. Heart Fail.* **18**, 744–758, https://doi.org/10.1002/ejhf.600

Clinical Science (2023) **137** 47–63
https://doi.org/10.1042/CS20220513

14 Charloux, A., Piquard, F., Doutreleau, S., Brandenberger, G. and Geny, B. (2003) Mechanisms of renal hyporesponsiveness to ANP in heart failure. *Eur. J. Clin. Invest.* **33**, 769–778, https://doi.org/10.1046/j.1365-2362.2003.01222.x
15 Ismail, Y., Kasmikha, Z., Green, H.L. and McCullough, P.A. (2012) Cardio-renal syndrome type 1: epidemiology, pathophysiology, and treatment. *Seminars in nephrology*, pp. 18–25, Elsevier, https://doi.org/10.1016/j.semnephrol.2011.11.003
16 Mezhonov, E.M., Vialkina, I.A., Vakulchik, K.A. and Shalaev, S.V. (2021) Acute kidney injury in patients with ST-segment elevation acute myocardial infarction: Predictors and outcomes. *Saudi J. Kidney Dis. Transpl.* **32**, 318–327, https://doi.org/10.4103/1319-2442.335442
17 Brar, A. and Markell, M. (2019) Impact of gender and gender disparities in patients with kidney disease. *Curr. Opin. Nephrol. Hypertens.* **28**, 178–182, https://doi.org/10.1097/MNH.0000000000000482
18 Lima-Posada, I., Portas-Cortes, C., Perez-Villalva, R., Fontana, F., Rodriguez-Romo, R., Prieto, R. et al. (2017) Gender differences in the acute kidney injury to chronic kidney disease transition. *Sci. Rep.* **7**, 12270, https://doi.org/10.1038/s41598-017-09630-2
19 Kanic, V., Vollrath, M., Kompara, G., Suran, D. and Hojs, R. (2018) Women and acute kidney injury in myocardial infarction. *J. Nephrol.* **31**, 713–719, https://doi.org/10.1007/s40620-018-0504-4
20 Ly, J.D., Grubb, D.R. and Lawen, A. (2003) The mitochondrial membrane potential (deltapsi(m)) in apoptosis; an update. *Apoptosis* **8**, 115–128, https://doi.org/10.1023/A:1022945107762
21 Seppi, T., Prajczer, S., Dorler, M.M., Eiter, O., Hekl, D., Nevinny-Stickel, M. et al. (2016) Sex differences in renal proximal tubular cell homeostasis. *J. Am. Soc. Nephrol.* **27**, 3051–3062, https://doi.org/10.1681/ASN.2015080886
22 Petrica, L., Gluhovschi, C. and Velciov, S. (2012) Chronic kidney disease and the involvement of estrogen hormones in its pathogenesis and progression. *Rom. J. Intern. Med.* **50**, 135–144
23 National Research Council Committee for the Update of the Guide for the, C., and A. Use of Laboratory (2011) The National Academies Collection: Reports funded by National Institutes of Health. *Guide for the Care and Use of Laboratory Animals*, 8th ed., National Academies Press (US) National Academy of Sciences, Washington (DC)
24 Welinder, C. and Ekblad, L. (2011) Coomassie staining as loading control in Western blot analysis. *J. Proteome Res.* **10**, 1416–1419, https://doi.org/10.1021/pr1011476
25 Aldridge, G.M., Podrebarac, D.M., Greenough, W.T. and Weiler, I.J. (2008) The use of total protein stains as loading controls: an alternative to high-abundance single-protein controls in semi-quantitative immunoblotting. *J. Neurosci. Methods* **172**, 250–254, https://doi.org/10.1016/j.jneumeth.2008.05.003
26 Srivastava, S. (2016) Emerging therapeutic roles for NAD(+) metabolism in mitochondrial and age-related disorders. *Clin. Transl. Med.* **5**, 25, https://doi.org/10.1186/s40169-016-0104-7
27 Xie, N., Zhang, L., Gao, W., Huang, C., Huber, P.E., Zhou, X. et al. (2020) NAD(+) metabolism: pathophysiologic mechanisms and therapeutic potential. *Signal Transduct. Target Ther.* **5**, 227, https://doi.org/10.1038/s41392-020-00311-7
28 Wang, C., Pei, Y.Y., Ma, Y.H., Ma, X.L., Liu, Z.W., Zhu, J.H. et al. (2019) Risk factors for acute kidney injury in patients with acute myocardial infarction. *Chin. Med. J. (Engl.)* **132**, 1660–1665, https://doi.org/10.1097/CM9.0000000000000293
29 Windt, W.A., Eijkelkamp, W.B., Henning, R.H., Kluppel, A.C., de Graeff, P.A., Hillege, H.L. et al. (2006) Renal damage after myocardial infarction is prevented by renin-angiotensin-aldosterone-system intervention. *J. Am. Soc. Nephrol.* **17**, 3059–3066, https://doi.org/10.1681/ASN.2006030209
30 Fan, Z., Li, Y., Ji, H. and Jian, X. (2018) Nomogram model to predict cardiorenal syndrome type 1 in patients with acute heart failure. *Kidney Blood Press. Res.* **43**, 1832–1841, https://doi.org/10.1159/000495815
31 Habeichi, N.J., Mroueh, A., Kaplan, A., Ghali, R., Al-Awassi, H., Tannous, C. et al. (2020) Sex-based differences in myocardial infarction-induced kidney damage following cigarette smoking exposure: more renal protection in premenopausal female mice. *Biosci. Rep.* **40**, BSR20193229, https://doi.org/10.1042/BSR20193229
32 Cavasin, M.A., Sankey, S.S., Yu, A.-L., Menon, S. and Yang, X.-P. (2003) Estrogen and testosterone have opposing effects on chronic cardiac remodeling and function in mice with myocardial infarction. *Am. J. Physiol.-Heart Circulatory Physiol.* **284**, H1560–H1569, https://doi.org/10.1152/ajpheart.01087.2002
33 Mitoff, P.R., Gam, D., Ivanov, J., Al-hesayen, A., Azevedo, E.R., Newton, G.E. et al. (2011) Cardiac-specific sympathetic activation in men and women with and without heart failure. *Heart* **97**, 382–387, https://doi.org/10.1136/hrt.2010.199760
34 Cingolani, O.H., Kaludercic, N. and Paolocci, N. (2011) Sexual dimorphism in cardiac norepinephrine spillover: a NET difference. *Heart* **97**, 347–349, https://doi.org/10.1136/hrt.2010.217133
35 Du, X.J., Riemersma, R.A. and Dart, A.M. (1995) Cardiovascular protection by oestrogen is partly mediated through modulation of autonomic nervous function. *Cardiovasc. Res.* **30**, 161–165, https://doi.org/10.1016/S0008-6363(95)00030-5
36 Bejjani, A.T., Saab, S.A., Muhieddine, D.H., Habeichi, N.J., Booz, G.W. and Zouein, F.A. (2019) Spatiotemporal dynamics of immune cells in early left venticular remodeling after acute myocardial infarction in mice. *J. Cardiovasc. Pharmacol.* **75** (112-122)
37 Halawa, B., Salomon, P., Jolda-Mydlowska, B. and Zysko, D. (1999) Levels of tumor necrosis factor (TNF-alpha) and interleukin 6 (IL-6) in serum of patients with acute myocardial infarction. *Pol. Arch. Med. Wewn.* **101**, 197–203
38 Kobeissy, F., Shaito, A., Kaplan, A., Baki, L., Hayek, H., Dagher-Hamalian, C. et al. (2017) Acute exposure to cigarette smoking followed by myocardial infarction aggravates renal damage in an in vivo mouse model. *Oxid. Med. Cell Longev.* **2017**, 5135241, https://doi.org/10.1155/2017/5135241
39 Sasaki, T., Tsuboi, N., Haruhara, K., Okabayashi, Y., Kanzaki, G., Koike, K. et al. (2018) Bowman capsule volume and related factors in adults with normal renal function. *Kidney Int. Rep.* **3**, 314–320, https://doi.org/10.1016/j.ekir.2017.10.007
40 Munshi, R., Hsu, C. and Himmelfarb, J. (2011) Advances in understanding ischemic acute kidney injury. *BMC Med.* **9**, 11, https://doi.org/10.1186/1741-7015-9-11

41 Lekawanvijit, S., Kompa, A.R., Zhang, Y., Wang, B.H., Kelly, D.J. and Krum, H. (2012) Myocardial infarction impairs renal function, induces renal interstitial fibrosis, and increases renal KIM-1 expression: implications for cardiorenal syndrome. *Am. J. Physiol. Heart Circ. Physiol.* **302**, H1884–H1893, https://doi.org/10.1152/ajpheart.00967.2011
42 Liu, P., Zhang, Z. and Li, Y. (2021) Relevance of the pyroptosis-related inflammasome pathway in the pathogenesis of diabetic kidney disease. *Front. Immunol.* **12**, 603416, https://doi.org/10.3389/fimmu.2021.603416
43 Lei, Y., Devarapu, S.K., Motrapu, M., Cohen, C.D., Lindenmeyer, M.T., Moll, S. et al. (2019) Interleukin-1beta inhibition for chronic kidney disease in obese mice with Type 2 diabetes. *Front. Immunol.* **10**, 1223, https://doi.org/10.3389/fimmu.2019.01223
44 Faubel, S., Lewis, E.C., Reznikov, L., Ljubanovic, D., Hoke, T.S., Somerset, H. et al. (2007) Cisplatin-induced acute renal failure is associated with an increase in the cytokines interleukin (IL)-1β, IL-18, IL-6, and neutrophil infiltration in the kidney. *J. Pharmacol. Exp. Ther.* **322**, 8–15, https://doi.org/10.1124/jpet.107.119792
45 Yang, B., El Nahas, A.M., Thomas, G.L., Haylor, J.L., Watson, P.F., Wagner, B. et al. (2001) Caspase-3 and apoptosis in experimental chronic renal scarring. *Kidney Int.* **60**, 1765–1776, https://doi.org/10.1046/j.1523-1755.2001.00013.x
46 Zhang, M.-Z., Wang, X., Wang, Y., Niu, A., Wang, S., Zou, C. et al. (2017) IL-4/IL-13–mediated polarization of renal macrophages/dendritic cells to an M2a phenotype is essential for recovery from acute kidney injury. *Kidney Int.* **91**, 375–386, https://doi.org/10.1016/j.kint.2016.08.020
47 Kim, A.H., Chung, J.J., Akilesh, S., Koziell, A., Jain, S., Hodgin, J.B. et al. (2017) B cell-derived IL-4 acts on podocytes to induce proteinuria and foot process effacement. *JCI Insight* **2**, https://doi.org/10.1172/jci.insight.81836
48 Giannandrea, M. and Parks, W.C. (2014) Diverse functions of matrix metalloproteinases during fibrosis. *Dis. Model Mech.* **7**, 193–203, https://doi.org/10.1242/dmm.012062
49 Zuo, Z., Huang, P., Jiang, Y., Zhang, Y. and Zhu, M. (2019) Acupuncture attenuates renal interstitial fibrosis via the TGF-beta/Smad pathway. *Mol. Med. Rep.* **20**, 2267–2275
50 Liu, N., Tolbert, E., Ponnusamy, M., Yan, H. and Zhuang, S. (2011) Delayed administration of suramin attenuates the progression of renal fibrosis in obstructive nephropathy. *J. Pharmacol. Exp. Ther.* **338**, 758–766, https://doi.org/10.1124/jpet.111.181727
51 Hu, N., Duan, J., Li, H., Wang, Y., Wang, F., Chu, J. et al. (2016) Hydroxysafflor yellow A ameliorates renal fibrosis by suppressing TGF-beta1-Induced epithelial-to-mesenchymal transition. *PLoS ONE* **11**, e0153409, https://doi.org/10.1371/journal.pone.0153409
52 Hershberger, K.A., Martin, A.S. and Hirschey, M.D. (2017) Role of NAD(+) and mitochondrial sirtuins in cardiac and renal diseases. *Nat. Rev. Nephrol.* **13**, 213–225, https://doi.org/10.1038/nrneph.2017.5
53 Ratajczak, J., Joffraud, M., Trammell, S.A., Ras, R., Canela, N., Boutant, M. et al. (2016) NRK1 controls nicotinamide mononucleotide and nicotinamide riboside metabolism in mammalian cells. *Nat. Commun.* **7**, 13103, https://doi.org/10.1038/ncomms13103
54 Zhang, D., Hu, X., Li, J., Liu, J., Baks-te Bulte, L., Wiersma, M. et al. (2019) DNA damage-induced PARP1 activation confers cardiomyocyte dysfunction through NAD+ depletion in experimental atrial fibrillation. *Nat. Commun.* **10**, 1307, https://doi.org/10.1038/s41467-019-09014-2
55 Ramsey, K.M., Mills, K.F., Satoh, A. and Imai, S. (2008) Age-associated loss of Sirt1-mediated enhancement of glucose-stimulated insulin secretion in beta cell-specific Sirt1-overexpressing (BESTO) mice. *Aging Cell* **7**, 78–88, https://doi.org/10.1111/j.1474-9726.2007.00355.x
56 Yoshino, J., Mills, K.F., Yoon, M.J. and Imai, S. (2011) Nicotinamide mononucleotide, a key NAD(+) intermediate, treats the pathophysiology of diet- and age-induced diabetes in mice. *Cell Metab.* **14**, 528–536, https://doi.org/10.1016/j.cmet.2011.08.014
57 Imai, S. and Guarente, L. (2014) NAD+ and sirtuins in aging and disease. *Trends Cell Biol.* **24**, 464–471, https://doi.org/10.1016/j.tcb.2014.04.002
58 Stein, L.R. and Imai, S.i. (2014) Specific ablation of Nampt in adult neural stem cells recapitulates their functional defects during aging. *EMBO J.* **33**, 1321–1340, https://doi.org/10.1002/embj.201386917
59 Kang, K.P., Lee, J.E., Lee, A.S., Jung, Y.J., Kim, D., Lee, S. et al. (2014) Effect of gender differences on the regulation of renal ischemia-reperfusion-induced inflammation in mice. *Mol. Med. Rep.* **9**, 2061–2068, https://doi.org/10.3892/mmr.2014.2089
60 Shawky, L.M. and Morsi, A.A. The effect of erythropoietin versus estrogen on the renal parenchyma of an animal model of renal ischemia reperfusion plus ovariectomy: comparative histomorphological study. *Int. J. Histol. Cytol.* **5**, 456–465
61 Annie, L., Gurusubramanian, G. and Roy, V.K. (2019) Estrogen and progesterone dependent expression of visfatin/NAMPT regulates proliferation and apoptosis in mice uterus during estrous cycle. *J. Steroid Biochem. Mol. Biol.* **185**, 225–236, https://doi.org/10.1016/j.jsbmb.2018.09.010
62 Stevens, L.A., Coresh, J., Greene, T. and Levey, A.S. (2006) Assessing kidney function–measured and estimated glomerular filtration rate. *N. Engl. J. Med.* **354**, 2473–2483, https://doi.org/10.1056/NEJMra054415
63 Shahbaz, H. and Gupta, M. (2019) Creatinine clearance. *StatPearls*, StatPearls Publishing
64 Kellum, J.A., Sileanu, F.E., Murugan, R., Lucko, N., Shaw, A.D. and Clermont, G. (2015) Classifying AKI by urine output versus serum creatinine level. *J. Am. Soc. Nephrol.* **26**, 2231–2238, https://doi.org/10.1681/ASN.2014070724
65 Cravedi, P. and Remuzzi, G. (2013) Pathophysiology of proteinuria and its value as an outcome measure in chronic kidney disease. *Br. J. Clin. Pharmacol.* **76**, 516–523
66 Hobeika, L., Hunt, K.J., Neely, B.A. and Arthur, J.M. (2015) Comparison of the rate of renal function decline in nonproteinuric patients with and without diabetes. *Am. J. Med. Sci.* **350**, 447–452, https://doi.org/10.1097/MAJ.0000000000000583

Supplement

Additional Methods

1. Echocardiography

Echocardiography was performed according to the American Society of Echocardiography guidelines, using a Vevo 2100™ High-Resolution Imaging System (Visual Sonics, Toronto, Canada). Mice were exposed to isoflurane (1.5-2% in oxygen) inhalation in order to induce general anesthesia. A heated electrical platform was used to maintain body temperature at 37°C, which was monitored by rectal thermostat. Body temperature, heart rate, and respiratory rate were continuously monitored throughout the procedure. Each animal was maintained for 5 min under anesthesia and on the heated platform in a supine position until stabilization of vital signs. B-mode and M-mode echocardiography images were obtained in the parasternal long-axis view in a supine position while the transducer was placed on the left thorax and ultrasound beam was directed at the mid-papillary muscle level. All images were acquired with heart rate between 400 and 500 BPM. Ejection fraction (EF) was measured at baseline, at day one, and right before sacrifice in all experimental groups.

2. Enzyme-linked immunosorbent assays (ELISAs)

2.1. Assessment of plasma tumor necrosis factor-alpha (TNF-α) levels. Plasma TNF-α was detected using an ELISA STEMCELL Technologies kit (#02030), according to the manufacturer's instructions. Plasma samples 1:1 were added to ELISA diluent to reach a total minimum volume of 250 µL. One hundred µL of diluted sample was loaded in duplicate in the ELISA strip plate pre-coated with capture antibodies specific for the cytokine TNF-α and incubated 2h at room temperature. Five rinses with 300 µL washing buffer were performed,

biotinylated detection antibody was added, followed by incubation for 1 h. After 5 washes (300 µL each), 100 µL/well diluted streptavidin horseradish peroxidase (SA-HRP) was added, and the plate incubated for 1 h at room temperature. Wells were washed, and 100 µL of 3,3',5,5'-tetramethylbenzidine (TMB) substrate was added to each well and the plate incubated at room temperature for 15 min. Finally, 100 µL/well of stopping solution was added and the absorbance measured at 450 nm in a microplate reader.

2.2. Assessment of plasma 17β estradiol. Levels of plasma 17β estradiol were measured using the ELISA Abcam kit (#108667) in order to verify that female mice were in the premenopausal phase (22) and to confirm success of ovariectomy **(Suppl. Table 1).** Twenty-five µL of samples were loaded in duplicate. Afterward, 17β estradiol-HRP conjugated was added, and the plate incubated for 2 h at room temperature. After 3 washes with 100 µL washing buffer, 100 µL/well of TMB substrate was added to all wells and the plate incubated at room temperature for 30 min. Finally, 100 µL stopping solution was added per well and absorbance measured at 450 nm in a microplate reader.

Female group	Plasma 17β estradiol levels (Mean ± SEM) pg/mL	P value
Control	32.219 ± 2.489	0.5525
FMI	34.742 ± 1.336	
FMIOVX	Under detection limit <10	

Suppl. Table 1: Plasma estrogen levels in female mice

3. Immunofluorescence (IF)

IF was performed to detect accumulation of α-smooth muscle actin (α-SMA) in kidney tissues. Unstained kidney slides were placed in antigen retrieval buffer for fifteen min at 95°C. Slides were washed 2x with Tris-buffered saline (TBS) with 0.025% Triton (TBS-T 0.025%), 5 min

each and incubated with 10% normal goat serum (NGS) + 1% bovine serum albumin (BSA) in TBS at room temperature for 2 h to block non-specific binding of α-SMA antibody. Incubation with α-SMA antibody (1:200, Abcam, ab5694) in TBS was performed overnight at 4°C, followed by two 5 min washes with TBS-T 0.025%. Kidney slides were incubated with the fluorescein isothiocyanate (FITC) conjugated secondary antibody (Abcam, ab97050) in TBS (1:100) for 1 h and washed 2x 5 min with TBS. Finally, DAPI was added and slides were washed 2x with phosphate-buffered saline (PBS), 5 min each time, and observed with a Zeiss Axio under 20x magnification.

4. Twenty-four hour urine collection

Mice of both sexes were individually housed in clean dry metabolic cages 24 hours before sacrifice with free access to water replacement pouches, in order to collect 24 hour urine. Urine samples were used to measure urine output, proteinuria, and creatinine clearance.

5. Proteinuria measurement

Proteinuria was measured using Bradford reagent in a 96-well plate. Briefly, protein standards were prepared with BSA ranging from 0.1-1.4 mg/ml. Five µL of the urine samples were added to separate wells in the 96-well plate followed by 250 µL of Bradford reagent and the plate incubated at room temperature for 30 min. Absorbance was measured at 595 nm.

6. Creatinine clearance determination

Creatinine concentration in plasma and urine samples was measured by the Jaffé-method using a Fluitest® CREA kit (Analyticon) according to the manufacturer's protocol. Creatinine clearance

(Crcl) was expressed as ml/min and obtained from the following equation: (concentration of urine creatinine (mg/mL) / concentration of plasma creatinine (mg/mL)) x urine volume (mL) in 24 hour.

Supplementary Figures

Total protein quantification

IL-1β and uncleaved caspase-3 protein levels were normalized to total protein (**Supplemental Figure 1A and 1A`**)

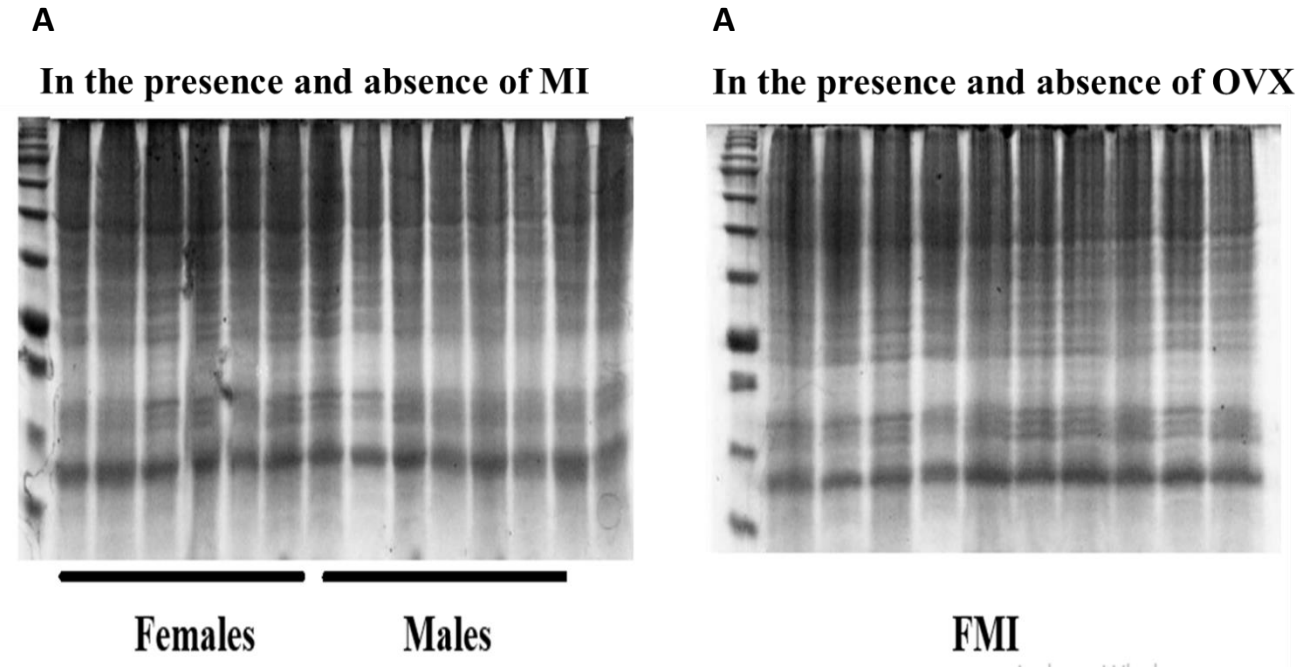

Supplemental Figure 1: Representative figure of total protein quantification using Coomassie blue in male and female MI mice in the presence and absence of MI (**1A)** and OVX (**1A`**); MI: Myocardial Infarction; OVX: Ovariectomy

The impact of MI and OVX on the accumulation of α-SMA in the kidneys

Supplemental Figure 2A shows an accumulation of α-SMA protein levels in the peritubular space in males post-MI, whereas no accumulation of α-SMA in the peritubular space in female mice following MI and OVX was observed **(2A`)**

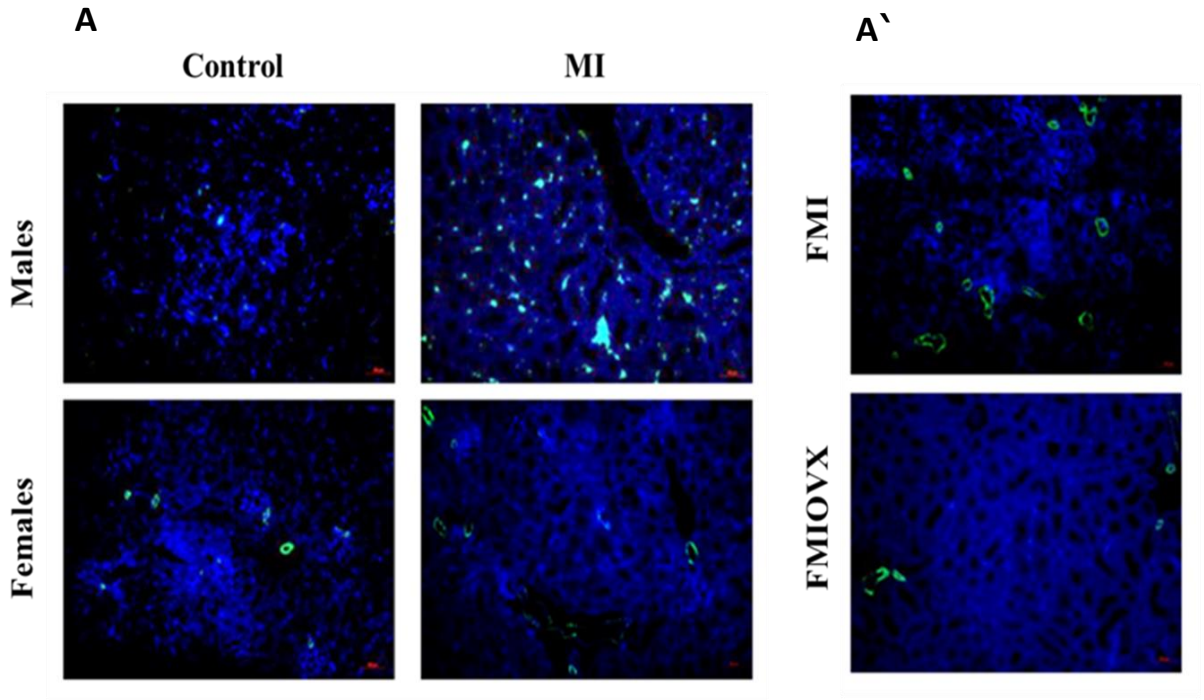

Supplemental Figure 2: Representative figure of IF shows an accumulation of α-SMA in the peritubular space of the kidneys in MI male mice, only. MI: Myocardial Infarction; OVX: Ovariectomy

Total protein quantification

IL-4 and α-SMA protein levels were normalized to total protein (**Supplemental Figures 3A and 3A`**)

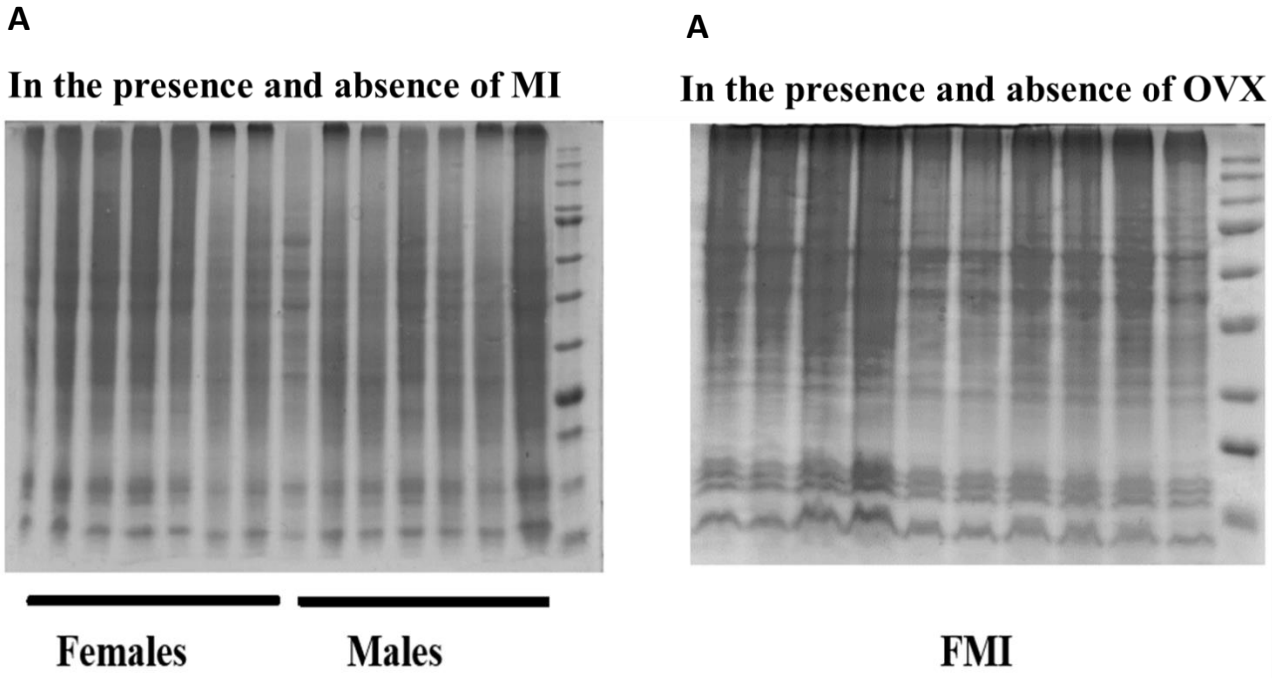

Supplemental Figure 3: Representative figure of total protein quantification using Coomassie blue in male and female MI mice in the presence and absence of MI (**3A**); and OVX (**3A`**); MI: Myocardial Infarction; OVX: Ovariectomy